Am J Cancer Res 2016;6(2):127-140
www.ajcr.us /ISSN:2156-6976/ajcr0017755

Review Article

MicroRNA-338-3p suppresses metastasis of lung cancer cells by targeting the EMT regulator Sox4

Yang Li, Peirui Chen, Lingling Zu, Bin Liu, Min Wang, Qinghua Zhou

Tianjin Key Laboratory of Lung Cancer Metastasis and Tumor Microenvironment, Tianjin Lung Cancer Institute, Tianjin Medical University General Hospital, Tianjin 300052, China

Received October 13, 2015; Accepted November 8, 2015; Epub January 15, 2016; Published February 1, 2016

Abstract: Metastasis remains the leading cause of the majority of cancer-related mortality. MicroRNAs (miRNAs) have frequently emerged as tumor metastatic regulator by acting on multiple signaling pathways. In the present study, we demonstrated that miR-338-3p was significantly downregulated in highly metastatic NSCLC cell lines and clinical metastatic tissues. Then, we found that introduction of miR-338-3p significantly suppressed the migration and invasion of lung cancer cells both in vitro and in vivo, suggesting that miR-338-3p may be a novel tumor suppressor. Further studies indicated that the EMT-related transcription factor Sox4 was one direct target gene of miR-338-3p, evidenced by the direct binding of miR-338-3p with the 3'untranslated region (3'UTR) of Sox4. Furthermore, miR-338-3p could decrease the expression of Sox4 both at mRNA and protein levels. Notably, the EMT marker E-cadherin or vimentin, a downstream regulator of Sox4, was also down-regulated or up-regulated upon miR-338-3p treatment. Additionally, over-expressing or silencing Sox4 could elevate or inhibit the migration and invasion of lung cancer cells, parallel to the effect of miR-338-3p on the lung cancer cells. Meanwhile, knockdown of Sox4 reversed the enhanced migration and invasion mediated by miR-338-3p. These results indicated that miR-338-3p suppressed the migration and invasion of NSCLC cells through targeting Sox4 involving in the EMT process. Thus, our finding provides new insight into the mechanism of NSCLC progression. Therapeutically, miR-338-3p may serve as a potential target in the treatment of human lung cancer.

Keywords: MiR-338-3p, metastasis, sox4, NSCLC

Introduction

Lung cancer, predominantly non-small cell lung cancer (NSCLC), remains the leading cause of cancer-related death worldwide [1]. In clinical, most lung cancer patients eventually suffered relapse and/or metastasis after complete excision of the cancer, even if they were just at stage IA [2]. In recent years, although the great progresses have been made, the molecular mechanisms of lung cancer relapse and metastasis are still poorly understood [3-5].

MicroRNAs (miRNAs) are an abundant class of small, non-coding RNAs, approximately 19-25 nucleotides. It negatively regulates gene expression at the post-transcription level by interacting with the 3'untranslated regions (3'-UTRs) of target mRNA. Emerging evidence indicates miRNAs are aberrant expressed in various tumors, and it can modulate tumor initiation and progression and function in tumor cell invasion and metastasis [6-8]. Furthermore, owing to their "fine-tuning" modulatory capabilities, miRNAs are emerging as key regulators in various signaling pathways involved in development and cancer progression [9].

MiR-338-3p is mapped to the seventh intron of apoptosis-associated tyrosine kinase (AATK) gene. MiR-338-3p could regulate its host gene AATK expression in rat neurons [10]. The miR-338-3p was first reported in prion-induced neurodegeneration as the expression of miR-338-3p is reduced in the brains of mice infected with mouseadapted scrape [11]. In the tumorigenesis, miR-338-3p is down regulated in gastric cancers [12], colorectal cancers [13] and lung cancer [14]. The biological targets of miR-338-3p have been partially identified, such as RAB14, HIF-1α, CyclinD1, ZEB2 and FOXP4 [12, 15-17]. However, little is known about the role

of miR-338-3p in lung cancer cells migration and invasion. This study provides the evidence for the role of miR-338-3p in lung cancer metastasis and partially expounds the molecular mechanism underlying the function.

Sex-determining region Y-box 4 (SOX4), which belongs to a member of the Sox family of transcription factors, play instrumental functions during embryonic development and cell fate specification in virtually all cells, tissues, and organ systems [18-20]. Furthermore, the accumulating evidence indicates that Sox4 is implicated in tumor progression, metastasis, and tumor cell proliferation, such as that Sox4 can increase esophageal tumor cells proliferation and invasion [21], and promote progression and epithelial-mesenchymal transition (EMT) of prostate cancer cells [22], and accelerate tumor growth in pancreatic cancer [23].

In this study, we investigated the biological functions and the mechanism of miR-338-3p in lung cancer metastasis. We found that miR-338-3p was down-regulated in metastatic lung cancer cell lines and clinical tissues, and miR-338-3p expression was associated with clinicopathologic characters in NSCLC. Furthermore, we identified that the EMT regulator Sox4 was one of direct target genes of miR-338-3p. MiR-338-3p was able to inhibit EMT and metastasis of NSCLC cells through paralyzing the function of Sox4. In addition, we found that miR-338-3p expression in lung cancer cells could be epigenetically inactivated by the oncogenic trimethylated histone H3Lys27 (H3K27me3). These results finally demonstrate that miR-338-3p is potentially a therapeutic target for NSCLC.

Materials and methods

Ethics statement

The study was approved by the Ethics Committee of Tianjin Medical University, China, and written informed consents were obtained from all studied patients.

Clinical specimens

A total of 90 cases of NSCLC specimens were obtained from General Hospital of Tianjin Medical University. All 90 patients hadn't received radiation therapy or chemotherapy prior to the surgery. Tissue samples for use were stored in liquid nitrogen. And stored at -80°C until RNA extraction. The tumors were classified according to World Health Organization classification. The study was approved by hospital ethical committee, and every patient had written informed consent. Clinicopathological information of the patients about age, sex, stage and lymph node metastasis was obtained from patient records, which were summarized in **Table 1**.

Cell culture and transfection

The sub-cell lines, high-metastatic L9981 and low-metastatic NL9980, were isolated and established from a human lung large cell carcinoma cell line [24]. The high-metastatic 95D and low-metastatic 95C were sublines of human giant-cell lung carcinoma cell line [25]. The NSCLC cell line YTMLC-9 [26] was established in our institute. These cell lines were cultured in RPMI-1640 medium supplemented with 10% calf serum (Invitrogen, USA), 100 IU/ml penicillin and 100 IU/ml streptomycin. The A549 cell line, purchased from the American Tissue Culture Collection (ATCC), cultured in DMEM medium supplemented with 10% fetal bovine serum, 100 U/mL penicillin and 100 U/mL streptomycin. These cell lines were grown at 37°C in a humidified atmosphere with 5% CO_2. For transfection, cells were cultured to 70% confluence and transfected with plasmids using Lipofectamine 2000 (Invitrogen, CA, USA) according to the manufacturer's recommendation.

Plasmid constructions

Genomic sequence of human miR-338-3p, including 200 bp flanking sequence, was amplified from human genome, then inserted into the BamHI/EcoRI site of the pcDNA3.1 vector (Invitrogen), named as pcDNA3.1-miR-338-3p. The full-length 3'untranslated region (3'UTR) of Sox4 was amplified from human genomic DNA, and was cloned into the downstream of the firefly luciferase coding region of pMIR-GLOTM Luciferase vector (Promega, USA). The recombined vector was named as pMIR-Sox4. Mutations of miR-338-3p binding sites were introduced by site-directed mutagenesis and the resulted vector was named pMIR-Sox4-Mut. Primers used for the constructions were listed in Table S1. All the constructions were confirmed by sequencing.

Table 1. Relationship between miR-338-3p expression and clinicopathological factors in 45 NSCLC patients

Factor	miR-338-3p Expression			Z value	*P* value
	Median	25%	75%		
Age					
<60	0.1388	0.0060	0.6124		
≥60	0.0656	0.0082	0.4031	-0.323	0.747
Gender					
Man	0.0878	0.0091	0.5211		
Woman	0.0132	0.0037	0.3843	-1.693	0.091
Smoking history					
Smoker	0.0332	0.0056	0.4986		
No smoker	0.0991	0.0080	0.5447	-1.215	0.224
Histology					
Squamous cancer	0.0397	0.0055	0.3995		
Adenocarcinoma	0.0698	0.0075	0.5087		
Large cell carcinoma	0.1696	0.0062	1.0000	1.426	0.49
Stage					
I+II	0.1953	0.0120	1.124		
III+IV	0.0104	0.0045	0.1742	-3.474	0.001
Lymph node status					
Negative	0.0124	0.0051	0.1787		
Positive	0.1696	0.0103	0.8274	-2.733	0.006

Quantitative real-time PCR

Quantitative RT-PCR was performed to validate the miRNA expression level. QRT-PCR was carried out using SYBR®Premix Ex TaqTM (Takara, Japan). PCR were carried out in triplicate and analyzed using the ABI Prism 7900HT fast real-time PCR system (Applied Biosystems, Life technologies, USA). The relative quantification values for each gene were calculated by the $2^{-\Delta\Delta Ct}$ method using U6 or GAPDH as an internal reference. All primers were shown in Table S1.

Cell migration assay

The migration ability was determined using wound-healing assay. Equivalent L9981 and A549 cells were plated into 12-well plates without antibiotics; cells were transfected with miR-338-3p mimic (miR-338-3p) or mimic control (NC). 24 h later, transfected cells were wounded with a sterile plastic 100 μl micropipette tip, the floating debris were washed with PBS and cultured in serum-free medium. Width of the wound was measured at different time points. 3-4 different locations were visualized and photographed under a phase-contrast inverted microscope.

Cell invasion assay

Boyden chamber assay was used to examine cell invasion capability. Cells were transfected with miR-338-3p mimic, mimic control, miR-338-3p inhibitor or inhibitor control (Ruibobio, Guangzhou, China). Sixteen hours later, transfected cells were trypsinized and resuspended, 1.0×10^4 cells in 200 μl RPMI-1640 medium were placed into the upper chambers (8-mm pore size; Millipore). The lower chambers were filled with 600 μl complete medium with 10% FBS. After incubation for 12 h at 37°C, non-invading cells were removed from the top of the chamber with a cotton swab. The invasion cells on the lower surface of the inserts were fixed and stained with 0.1% crystal violet, and five random fields for each insert were counted at 200× magnifications.

Proliferation assay

MTT assay was used to analyze cell proliferation. L9981 and A549 cells were transfected with either miR-338-3p mimic (miR-338-3p) or mimic control (NC). After 24 h transfection, cells were seeded into 96-well plate at 5.0×10^3 cells/ml and continue cultured for 24, 48, 72, 96 h, and 120 h, respectively. At each time point, 10 μl MTT reagent (5 mg/ml, Sigma) was added to each well, successive incubated for 4 h at 37°C. The supernatant was removed and 200 μl DMSO (Invitrogen) was added to dissolve the formazan crystals for 30 min. Spectrometric absorbance at a wavelength of 570 nm was measured on microplate reader (Spectra Max M5, MD, USA). Each sample was tested in triplicate and all experiments were performed three times.

In vivo assay

For the in vivo metastasis assays, the stable cell line L9981-luc-miR-338-3p and control cell line L9981-luc-pcDNA3.1 were collected and suspended in 0.2 ml PBS for each mouse (four in each group, 6-8 weeks age), and the cells were injected into left side of the posterior flank of nude mouse. Thirty minutes after cell injection, luciferase substrate was added at a dose

of 150 mg/kg and live images of the mouse were obtained using an IVIS200 (Xenogene, USA). These data were classified as Day 0. Luciferase activity was measured every 7 days using the same protocol. Tumor growth was measured periodically. The fluorescence intensity was calculated using Plus Image-Pro software (Media Cybernetics, Bethesda, MD, USA).

Dual-luciferase reporter assay

Cells were seeded into 24-well plates and cotransfected with 200 ng of pMIR-Sox4 or pMIR-Sox4-Mut vector and 100 ng of miR-338-3p mimic or mimic control, and the pRL-TK plasmid (Promega, Madison, WI) which was used as internal normalization. After 48 h, cells were lysed using the lysis buffer (Promega). Luciferase reporter gene assay was implemented using the Dual-Luciferase Reporter Assay System (Promega) according to the manufacturer's instructions. All experiments were performed at least three times.

Western blotting

Cells were transfected with either miR-338-3p, pCMV-Tag-2b-Sox4 or small interfere RNA target Sox4 (si-SOX4). Total cell extracts prepared from cells using RIPA buffer (Beyotime, China), were resolved on 10% gradient SDS-polacrylamide gel and transferred NC membranes. Membranes were blocked for 1 hour in 5% skim milk in TBST and incubated with primary antibody overnight at 4°C, followed by the incubation with appropriate HRP-conjugated secondary antibody at optimized concentration. The primary antibodies used in this study were as follows: anti-Sox4 antibody (1:1000, Santa Cruz), anti-E-cadherin antibody (1:1000, Santa Cruz), anti-vimentin antibody (1:1000, Santa Cruz) and anti-β-actin antibody (1:5000, CST). The densitometry of Western blot results was measured using ImageJ software.

ChIP assay

The cells were crosslinked and processed according to the Chromatin Immunoprecipitation (ChIP) Assay Kit (Invitrogen) protocol. Antibodies to H3K27me3 ((Invitrogen) were used at 10 μg per immunoprecipitation reaction respectively. ChIP results were analyzed by real-time PCR. All primers sequences were shown in Table S1.

Statistical analysis

The data were presented as mean ± standard deviation (SD). MiR-338-3p expression in 45 pairs of primary NSCLC tissues and corresponding lymph metastatic tissues was compared by Wilcoxon signed-rank test. Mann-Whitney test was used to analyze the relationship between miR-338-3p expression levels and clinicopathologic characters. T-test was used to determine the significant differences between control and treatment groups. Statistical analysis was performed using SPSS15.0 software, and $P<0.05$ was considered to be a statistically significant difference.

Results

MiR-338-3p is down-regulated in highly metastatic lung cancer cells and tissue specimens

We firstly evaluated the expression of miR-338-3p by qRT-PCR in six NSCLC cell lines with distinct metastatic capacities. We found that miR-338-3p levels exhibited a varying pattern in these cell lines. Notably, miR-338-3p expression was dramatically diminished in highly metastatic L9981 and 95D cells compared with their counterparts, which are the poorly metastatic NL9980 or 95C cell lines, respectively (**Figure 1A**). Furthermore, we examined the miR-338-3p expression in 45 paired clinical primary lung cancer tissues and corresponding metastatic lymph node cancer tissue samples. Tissues from the lymph metastases exhibited a significant lower miR-338-3p levels (**Figure 1B**, $P<0.001$, Wilcoxon signed-rank test) compared with their primary tumors. In addition, we analyzed the clinicopathological features of patients with NSCLC, the results showed that the expression level of miR-338-3p was associated with the pathological stage (**Table 1**, $P = 0.001$) and lymph node status (**Table 1**, $P = 0.006$). Taken together, these results suggest a possible link between down-regulation of miR-338-3p and metastasis of human lung cancer.

Downregulation of miR-338-3p promotes the growth, migration and invasion of NSCLC cells in vitro

Next, we tested the functional significance of miR-338-3p in NSCLC cells. MiR-338-3p lower expressed L9981 and A549 cells were transfected with miR-338-3p mimic (miR-338-3p) or

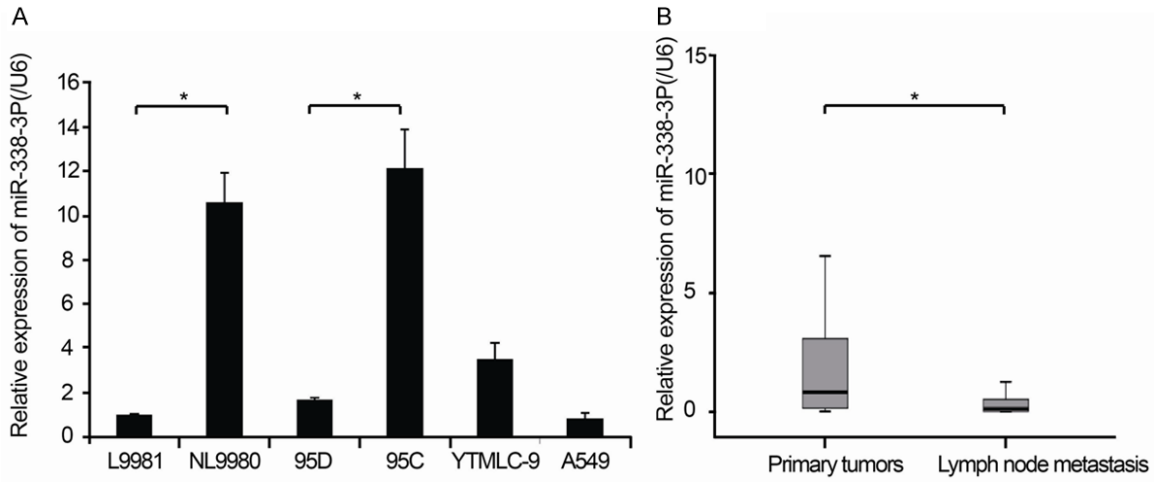

Figure 1. MiR-338-3p is frequently down-regulated in highly metastatic lung cancer cells and tissue specimens. A. The relative mRNA levels of miR-338-3p were detected by qRT-PCR and normalized against an endogenous control (U6 RNA) in several lung cancer cell lines with distinct metastatic ability. Data are reported as mean ± SD for three independent experiments (*P<0.05, t-test). B. qRT-PCR analysis of miR-338-3p expression in 45 pairs of primary NSCLC tissues and their corresponding lymph node metastases. (*P<0.05, Wilcoxon signed-rank test).

mimics control (NC), then wound healing assay was used to examine the cell migration ability. The results showed that the over expression of miR-338-3p significantly inhibited cell migration, compared to the control group (**Figure 2A**). Furthermore, we performed the Boyden chamber assay to investigate the effect of miR-338-3p on cell invasion. As shown in **Figure 2B** and **2C**, when transfected with miR-338-3p mimics, the invasion ability of L9981 and A549 cells was decreased, compared to the control group. However, the cells showed an increased invasion upon the treatment of miR-338-3p inhibitor (**Figure 2B**, **2C**). Additionally, we investigated the effect of miR-338-3p on cell proliferation by MTT assay. As shown in **Figure 2D**, when transfected with miR-338-3p mimics, the proliferation ability of L9981 and A549 cells was down-regulated compared to the control group. Taken together, the data strongly suggest that miR-338-3p can suppress the growth, migration and invasion of NSCLC cells *in vitro*.

Downregulation of miR-338-3p contributes to NSCLC progression in nude mouse xenograft model

To further confirm whether miR-338-3p could suppress metastatic behaviors *in vivo,* we established a miR-338-3p over-expressed L9981-luc-miR-338-3p (miR-338-3p) cell line and another L9981-luc-pcDNA3.1 cell line as negative control (NC). The cells were injected into mice and the fluorescence intensity was measured every one week until the forth week. The results showed that the fluorescence value of mice in the miR-338-3p overexpressed group was remarkably lower compared with the negative control group (**Figure 3A**). Additionally, Lung metastases fluorescence value of tumor-bearing mice in vitro was used to investigate the effect of miR-338-3p on metastasis. Compared with control group, the fluorescence value in miR-338-3p overexpressed group was lower (P<0.001) (**Figure 3B**). The results indicate that miR-338-3p significantly inhibits the tumorigenicity and metastasis of L9981 cells in the nude mouse xenograft model.

MiR-338-3p directly inhibits the expression of Sox4 through its 3'UTR and regulates the EMT of NSCLC cells

To gain further insight into the underlying molecular mechanism by which miR-338-3p suppresses migration and invasion of NSCLC cells, we searched for the putative genes targeted by miR-338-3p using biological target prediction softwares TargestScan, miRanda and PicTar. Among these genes, we were particularly interested in the gene encoding sex-determining region Y-box 4 (Sox4) because of its positive roles in cancer progression and invasion, and it harbored a potential miR-338-

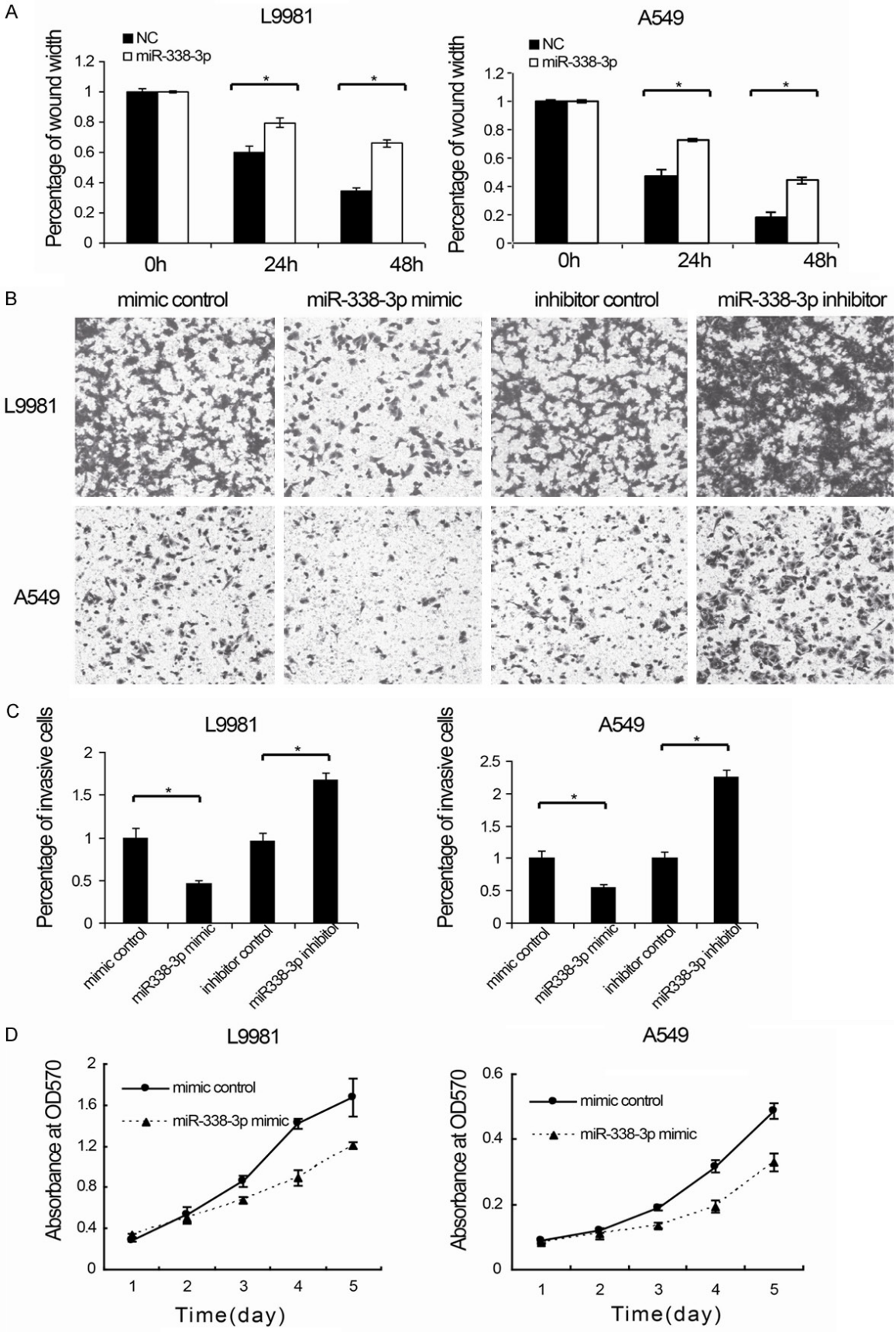
A
L9981
A549
NC
miR-338-3p
Percentage of wound width
0h
24h
48h
B
mimic control
miR-338-3p mimic
inhibitor control
miR-338-3p inhibitor
L9981
A549
C
L9981
A549
Percentage of invasive cells
mimic control
miR338-3p mimic
inhibitor control
miR338-3p inhibitor
D
L9981
A549
Absorbance at OD570
mimic control
miR-338-3p mimic
Time(day)

Figure 2. MiR-338-3p is able to inhibite the growth, migration and invasion of NSCLC cells in vitro. A. The wound healing was used to detected the migration ability of L9981 and A549 cells, respectively. B, C. Boyden chamber assay was employed to examine the invasion ability of L9981 and A549 cells, respectively. The results were from three independent experiments. The migratory cell number in each group was normalized to the control. Cells were transfected with miR-338-3p mimic or mimics control, and miR-338-3p inhibitor or inhibitor control. D. MTT assay was used to examine the proliferation ability of L9981 and A549 cells, respectively. Cells were transfected with miR-338-3p mimic or mimics control.

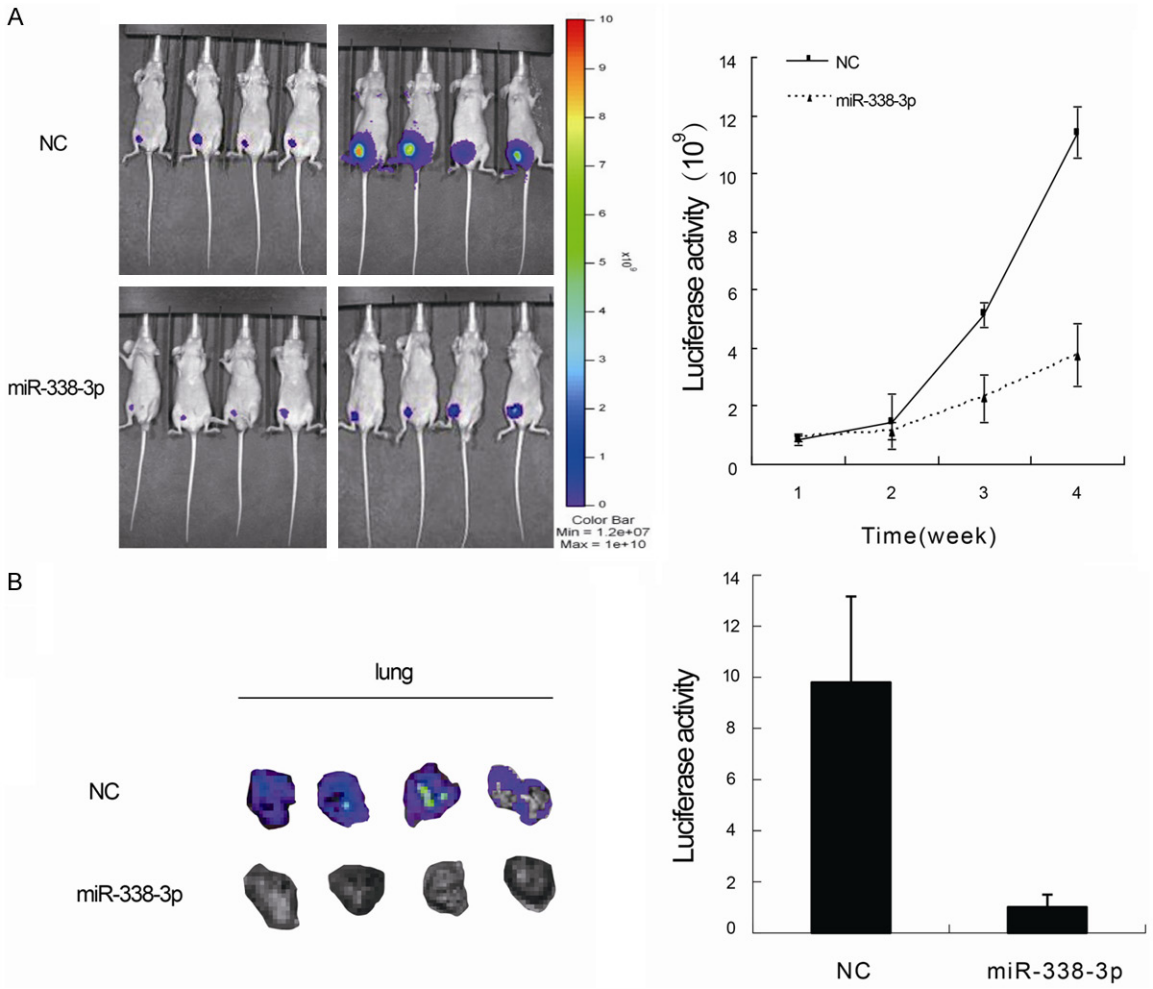

Figure 3. Downregulation of miR-338-3p contributes to NSCLC progression in vivo. The miR-338-3p overexpressed L9981-luc-miR-338-3p cells (miR-338-3p) and negative control cells L9981-luc-pcDNA3.1 (NC) were injected into the mice (4/group). A. Representative images of tumors are shown in the left on the indicated days. And tumor growth curve in mice are shown in the right. Data are mean ± SD. B. Lung metastases luciferase imaging of tumor-bearing mouse in vitro. The intensity was measured on week 4, and the luciferase value of each group was shown in the right. The pseudo-color scale bars represent the intensity of light emission with different colors. Data are reported as mean ± SD (**P*<0.05, t-test).

3p binding site within its 3'UTR (**Figure 4A**). To detect whether Sox4 was regulated by miR-338-3p, the wild type or mutant 3'UTR sequence of Sox4 was cloned into pMIR reporter vector, respectively, as shown in **Figure 4B**. The luciferase activity of pMIR-Sox4-3'UTR-wt construct was remarkably decreased upon the over-expression of miR-338-3p in L9981 cells, whereas its mutant counterpart was not (**Figure 4C**). In addition, the mRNA and protein levels of Sox4 in L9981 and 95D cells was damatically reduced after transfected miR-338-3p mimics (**Figure 4D-F**). Taken together, these data indicated that Sox4 is a direct target of miR-338-3p.

It is reported that Sox4 plays a critical role in EMT through suppressing E-cadherin or induc-

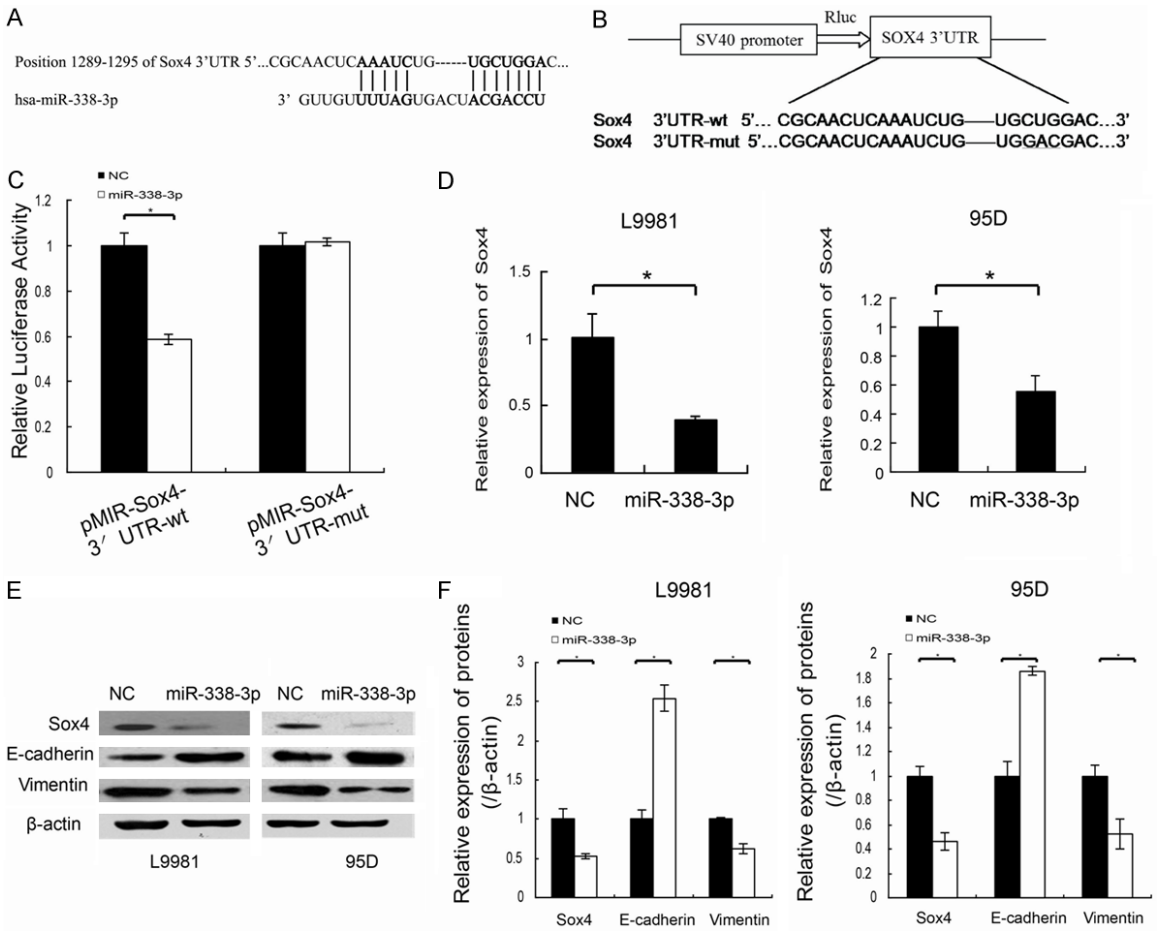

Figure 4. MiR-338-3p directly inhibits the expression of Sox4 through its 3'UTR and regulates the EMT of NSCLC cells. A. The miR-338-3p binding site predicted in the 3'UTR of Sox4 mRNA. B. Mutant was generated at the seed region of Sox4 3'UTR as indicated by the underline. A 3'UTR fragment of Sox4 mRNA containing wild-type or mutant of the miR-338-3p binding sequence was cloned into the downstream of the luciferase gene in pMIR vector. C. L9981 cells were transfected with pMIR reporter vectors containing either wild-type or mutant Sox4 3'UTR (indicated as pMIR-Sox4-3'UTR-wt and pMIR-Sox4-3'UTR-mut) with either miR-338-3p mimics (indicated as miR-338-3p) or miR-338-3p mimics control (indicated as NC). Luciferase activity was determined 48 h after transfection. D-F. The protein levels of Sox4, E-cadherin or vimentin was examined by western blot. E, F. Show the relative gray values of each band (normalized to β-actin). Protein bands from three independent western blot assays were quantified using Quantity One software (Bio-Rad, USA). Data are reported as mean ± SD (**P*<0.05, t-test).

ing vimentin expression in human cancer [27, 28]. To further determine that Sox4 acted as a target of miR-338-3p, we investigated the effect of miR-338-3p on those two downstream effectors of Sox4 by western blot. The results showed that the EMT maker E-cadherin or vimentin was dramatically up-regulated or down-regulated respectively upon the over-expression of miR-338-3p in L9981 and 95D cells (**Figure 4E**, **4F**). Taken together, these data show that miR-338-3p directly inhibits Sox4 expression via targeting its 3'UTR and induces EMT of NSCLC cells.

Sox4 contributes to miR-338-3p mediated migration, invasion and EMT of NSCLC cells

Then, we examined the expression of Sox4 in four NSCLC cell lines, as well as 45 pairs of primary lung cancer tissues and metastatic lymph node tissues. The data revealed that the protein level of Sox4 in the highly metastatic L9981 or 95D cells was markedly up-regulated, compared to the poorly metastatic NL9980 or 95C cells, respectively (**Figure 5A**). Furthermore, we also observed the same result that the mRNA levels of Sox4 in metastatic lymph node

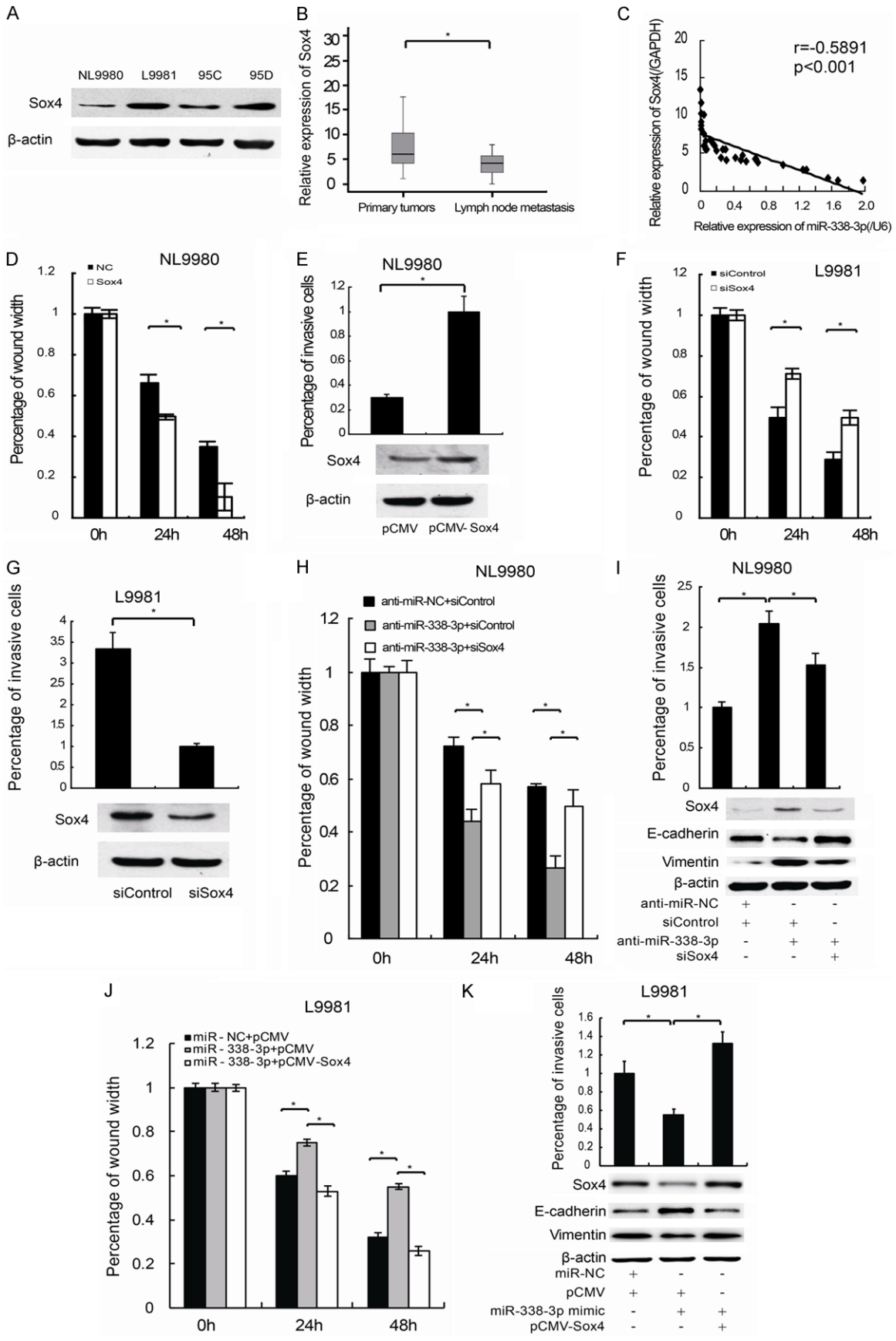
A
NL9980
L9981
95C
95D
Sox4
β-actin
B
Relative expression of Sox4
Primary tumors
Lymph node metastasis
C
r=-0.5891
p<0.001
Relative expression of Sox4/(GAPDH)
Relative expression of miR-338-3p/(U6)
D
NL9980
NC
Sox4
Percentage of wound width
0h
24h
48h
E
NL9980
Percentage of invasive cells
Sox4
β-actin
pCMV
pCMV- Sox4
F
L9981
siControl
siSox4
Percentage of wound width
G
L9981
Percentage of invasive cells
Sox4
β-actin
siControl
siSox4
H
NL9980
anti-miR-NC+siControl
anti-miR-338-3p+siControl
anti-miR-338-3p+siSox4
Percentage of wound width
I
NL9980
Percentage of invasive cells
Sox4
E-cadherin
Vimentin
β-actin
anti-miR-NC
siControl
anti-miR-338-3p
siSox4
J
L9981
miR - NC+pCMV
miR - 338-3p+pCMV
miR - 338-3p+pCMV-Sox4
Percentage of wound width
K
L9981
Percentage of invasive cells
Sox4
E-cadherin
Vimentin
β-actin
miR-NC
pCMV
miR-338-3p mimic
pCMV-Sox4

Figure 5. Sox4 inversely correlates with miR-338-3p expression and induces an EMT program in NSCLC. A. Sox4 expression was examined in NSCLC cells by Western blot method. B. The relative mRNA levels of Sox4 were detected in 45 paired NSCLC primary tissues and their lymph node metastasis counterparts. Sox4 expression in those tissues was compared by way of Wilcoxon signed-rank test (*P<0.05). C. Inverse correlation between miR-338-3p and Sox4 expression in NSCLC tissues. Sox4 expression was analyzed by qRT-PCR and normalized to GAPDH. The miR-338-3p expression was detected by qRT-PCR analysis and normalized to U6 expression. Statistical analysis was performed using Pearson's correlation coefficient (r = -0.5891, P<0.001). D, E. The cell migration or invasion ability was detected by wound healing or Boyden chamber assay in NL9980 cells transfected with pCMV or pCMV-Sox4 vectors, and Sox4 expression level was examined by Western blot. (*P<0.05, t-test). F, G. The effect of Sox4 knockdown on the cell migration or invasion was assessed in NL9981 cells by wound healing or Boyden chamber assay, respectively. Additionally, the silencing efficiency of Sox4 by siRNA was examined by Western blot. (*P<0.05, t-test). H-K. The wound healing or Boyden chamber assay was used to detect the migration or invasion ability of NL9980 cells with different treatments, respectively. Additionally, the protein levels of Sox4, E-cadherin or vimentin was examined by western blot. (*P<0.05, t-test).

tissues was up-regulated, compared with the primary lung cancer tissues (**Figure 5B**). Notably, the expression of Sox4 displayed a significant reverse correlation with miR-338-3p in NSCLC tissues (**Figure 5C**). Next, we investigated whether Sox4 contributed to the migration and invasion of NSCLC cells. Ectopic expression of Sox4 in NL9980 cells significantly promoted cells migration and invasion (**Figure 5D**, **5E**), however, silencing Sox4 by siRNAs in L9981 cells resulted in decreased migration and invasion ability of the cells (**Figure 5F**, **5G**), revealing its positive roles in the contribution of NSCLC cells migration and invasion. Meanwhile, the transfecting or silencing efficiency of Sox4 in the cells was detected by western blot (**Figure 5E** and **5G**, lower).

Then, because Sox4 is able to promote migration, invasion and EMT of NSCLC cells, and miR-338-3p can regulate the expression of Sox4, we investigated whether the functional effect of miR-338-3p on NSCLC cells was dependent on Sox4. To answer this question, we performed some functional experiments that was shown in **Figure 5H-K**, transfected miR-338-3p inhibitor into NL9980 cells resulted in an increase of cells migration and invasion, whereas silence of Sox4 by siRNAs partially weakened the enhancement (**Figure 5H** and **5I**). And we also found the similar results that over-expression of Sox4 could reverse the decreased migration and invasion abitily induced by miR-338-3p mimics in L9981 cells (**Figure 5J** and **5K**). In parallel, the protein level of Sox4 was determined by western blot (**Figure 5I** and **5K**, lower).

Meanwhile, the EMT maker E-cadherin and vimentin were examined by western blot. As shown in **Figure 5I**, the expression level of E-cadherin and vimentin were markedly down-regulated or up-regulated when NL9980 cells transfected with miR-338-3p inhibitor. While knockdown of Sox4, down-regulated E-cadherin and up-regulated vimentin expression induced by miR-338-3p was reversed. The results showed that Sox4 could contribute to miR-338-3p mediated EMT in NL9980 cells. The consistent results were observed in L9981 cells (**Figure 5K**, lower). Collectively, these results suggest that Sox4 is a functional target of miR-338-3p, which is responsible for miR-338-3p mediated NSCLC cells migration, invasion and EMT phenotype.

Epigenetic repression of miR-338-3p expression by histone modifications in NSCLC cells

The mechanism, by which miR-338-3p is down-regulated in NSCLC, is currently unknown, but one possibility is that its down-regulation might be caused by aberrant epigenetic events. As we known, miR-338-3p has been mapped to the seventh intron of AATK on chromosome 11, and previous studies involving the genome-scale analysis of transcription factor binding and histone modifications predict that these miRNAs share a common promoter with their host gene, AATK. So we detected the DNA methylation and H3K27 methylation on AATK/miR-338-3p promoter reagion. Then, A549 cells were treated with epigenetic drugs TSA(T), DZNep(D) respectively, or in combination for 48 h. The results showed that miR-338-3p expresssion was up-regulated after epigenetic drug treatment, especially T and D combination group (**Figure 6A**). So we speculated that miR-338-3p might be regulated by epigenetic events. Next, we examined H3K27me3 expression in AATK promoter reagion by ChIP analysis. As **Figure 6C** shown, miR-338-3p promoter exist H3K27me3 expression. Additionally,

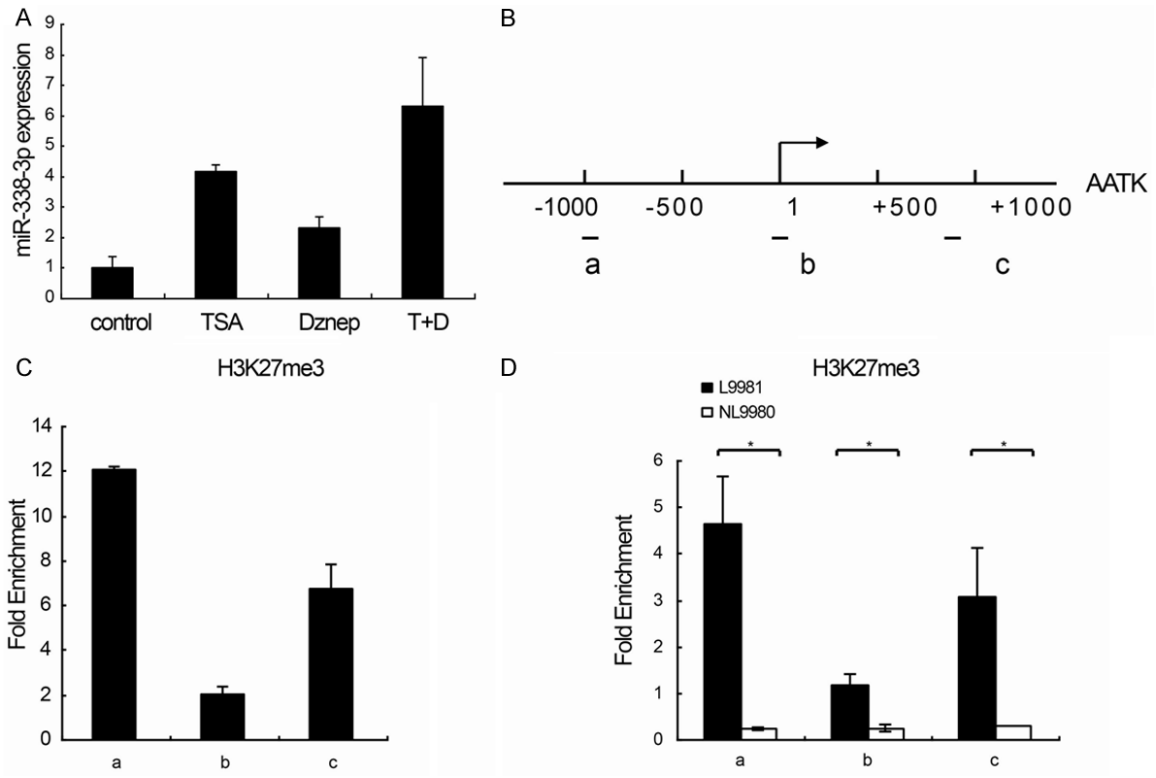

Figure 6. miR-338-3p is epigenetically repressed in lung cancer cells through histone methylation. A. The miR-338-3p expression was detected by qRT-PCR in A549 cells with TSA (100 nM), DZNep (5 mM) alone, or in combination for 48 h. B. The positions of examined DNA fragments are indicated by a, b, and c. C. H3K27me3 ChIP analysis at miR-338-3p/AATK locus in A549 cells. D. H3K27me3 ChIP analysis at miR-338-3p/AATK locus in NL9980 and L9981 cells.

H3K27me3 expression was also examined in one pair NSCLC cell lines with different metastatic ability. The results showed that H3K27me3 expression in highly metastatic L9981 cells was remarkably higher than that in poorly metastatic NL9980 cells (**Figure 6D**). This finding was consistent with the much lower expression of miR-338-3p in L9981 cells. Furthermore, we also found that DNA hypermethylation was not involved in miR-338-3p repression in NSCLC cells (Data is not displayed). These results indicate that histone methylation but not DNA methyation may be one reason for low-expression of miR-338-3p in lung cancer cells.

Discussion

Growing evidence has indicated that miRNAs play a crucial role in tumorigenesis and tumor progression [2-4]. Therefore it is important to identify tumor-related miRNAs and their target genes to understand their roles in tumor progression. Several miRNAs have been reported to be dysregulated in NSCLC [3-5]. You JC, et, al. found that miR-132 could inhibit the invasion of NSCLC cells by targeting ZEB2 [29]. Also, Boning Liu, et al. reported that miR-26a might promote metastasis of lung cancer cells through activating AKT by targeting PTEN [30]. MiR-338-3p was abbrent expressed in various cancers, such as gastric cancers [12], colorectal cancers [13] and non-small cell lung cancer [14]. Recently, Sun J, et al. found that down-regulated miR-338-3p significantly enhanced proliferation and suppressed apoptosis by targeting RAB 14 in NSCLC cells [14]. But, so far it is little known that the role of miR-338-3p in lung cancer cells migration and invasion. In the present study, we are interested in the potential role of miR-338-3p in the metastasis of NSCLC cells.

In this study, we found that miR-338-3p was frequently down-regulated in highly metastatic NSCLC cell lines and tissue specimens. Furthermore, statistical analysis revealed that miR-338-3p was correlated with advanced

pathological stage, and lymph node metastasis in NSCLC. Thus, we supposed that miR-338-3p could be a novel tumor suppressor miRNA and its dysregulation might involve in initial tumorigenesis and the advanced progress of human lung cancer. It was consistant with the present report [14]. For the mechanism involving miR-338-3p down-regulation, we found that histone H3 lys27 (H3K27me3) activated in the promoter region was responsible for the reduced expression of miR-338-3p in NSCLC. However, Pu Li, et al. found that the reduced expressions of miR-338-3p may be caused by DNA methylation in gastric cancer [31]. This may be due to the regulation of miR-338-3p present tissue specificity.

In addition, we investigated the role of miR-338-3p in NSCLC biological function. Our data showed that the re-introduction of miR-338-3p dramatically suppressed lung cancer tumorigenesis and metastasis both *in vitro* and *in vivo*. Therefore, we speculated that down-regulation of miR-338-3p could contribute to the growth and metastasis of cancer and consequently facilitated to the advanced development of NSCLC. A single miRNA can modulate a signaling network by targeting genes with multiple functions. Several miR-338-3p targets have been identified in different cell context and organs, such as, FOXP4 was found to be a target of miR-338-3p, which mediated an effect on cell proliferation in hepatocellular carcinoma [17]. Fu X, et al., indicated that miR-338-3p could induce a G1/S phase arrest by directly targeting CyclinD1 [15]. MiR-338-3p directly target smoothened to inhibit colorectal cancer cells migration and invasion ability [32]. Our present study found that Sox4 was a functional target of miR-338-3p by luciferase reporter gene assays and western blot.

Sox4 is a member of the Sox (SRY-related HMG-box) family of transcription factors, is overexpressed in several human cancers, including prostate cancer, esophageal cancer, breast cancer and non-small cell lung cancer. It is closely correlated with tumor invasion and metastasis and is also one of members of EMT-transcriptional inducers [27, 28, 33]. EMT is a key developmental program that is often activated during cancer progression and may promote resistance to therapy [34-36]. Zhang et al. [37] showed that overexpression of Sox4 in human mammary epithelial cells led to the acquisition of mesenchymal traits, and enhanced cell migration and invasion. Furthermore, Sox4 positively regulated the expression of known EMT inducers and activated the TGF-β pathway to contribute to EMT [33]. To date, EMT is an attractive target for therapeutic interventions, provides a new basis of the progression of carcinoma towards dedifferentiated and more malignant states [38, 39]. In our study, we found that Sox4 had a frequently high expression in metastatic NSCLC cells and clinical lymph node tissues. Sox4 expression inversely correlated with miR-338-3p expression in NSCLC tissue specimens. And Sox4 was responsible for miR-338-3p modulated migration and invasion of NSCLC cells. Notably, we found that E-cadherin or vimentin, the downstream effector of Sox4, was also down-regulated or up-regulated by miR-338-3p, indicating that miR-338-3p may exert functions in migration and invasion of NSCLC cells by modulating EMT progress.

In summary, we investigated the role of miR-338-3p in NSCLC progression and metastasis. Our study indicates that miR-338-3p may be a novel tumor suppressor miRNA. MiR-338-3p inhibits the migration and invasion of NSCLC cells through targeting the EMT regulator Sox4. Our data provide a new insight into the mechanism responsible for the development of human NSCLC. Therefore, targeting miR-338-3p could be a promising therapeutic strategy in NSCLC.

Acknowledgements

This study was supported by the grants from National Natural Science Foundation of China (No. 81201852), National 863 Program (No. 2012AA02A201, No. 2012AA02A502), and National 973 Program (No. 2010CB529405).

Disclosure of conflict of interest

None.

Address correspondence to: Dr. Qinghua Zhou, Tianjin Key Laboratory of Lung Cancer Metastasis and Tumor Microenvironment, Tianjin Lung Cancer Institute, Tianjin Medical University General Hospital, Tianjin 300052, China. Tel: +86 28 8629 8144; Fax: +86 28 8629 8164; E-mail: zhouqinghua_fys@126.com

References

[1] Travis WD. Pathology of lung cancer. Clin Chest Med 2002; 23: 65-81, viii.

[2] Chen T, Xu C, Chen J, Ding C, Xu Z, Li C and Zhao J. MicroRNA-203 inhibits cellular proliferation and invasion by targeting Bmi1 in non-small cell lung cancer. Oncol Lett 2015; 9: 2639-2646.

[3] Zhong C, Ding S, Xu Y and Huang H. MicroRNA-222 promotes human non-small cell lung cancer H460 growth by targeting p27. Int J Clin Exp Med 2015; 8: 5534-5540.

[4] Zhu D, Chen H, Yang X, Chen W, Wang L, Xu J and Yu L. Decreased microRNA-224 and its clinical significance in non-small cell lung cancer patients. Diagn Pathol 2014; 9: 198.

[5] Luo W, Huang B, Li Z, Li H, Sun L, Zhang Q, Qiu X and Wang E. MicroRNA-449a is downregulated in non-small cell lung cancer and inhibits migration and invasion by targeting c-Met. PLoS One 2013; 8: e64759.

[6] Lin Y, Wu J, Chen H, Mao Y, Liu Y, Mao Q, Yang K, Zheng X and Xie L. Cyclin-dependent kinase 4 is a novel target in micoRNA-195-mediated cell cycle arrest in bladder cancer cells. FEBS Lett 2012; 586: 442-447.

[7] Wang J, Gu Z, Ni P, Qiao Y, Chen C, Liu X, Lin J, Chen N and Fan Q. NF-kappaB P50/P65 hetero-dimer mediates differential regulation of CD166/ALCAM expression via interaction with micoRNA-9 after serum deprivation, providing evidence for a novel negative auto-regulatory loop. Nucleic Acids Res 2011; 39: 6440-6455.

[8] Xiao H, Zeng J, Li H, Chen K, Yu G, Hu J, Tang K, Zhou H, Huang Q, Li A, Li Y, Ye Z, Wang J and Xu H. MiR-1 downregulation correlates with poor survival in clear cell renal cell carcinoma where it interferes with cell cycle regulation and metastasis. Oncotarget 2015; 6: 13201-13215.

[9] Bartel DP. MicroRNAs: genomics, biogenesis, mechanism, and function. Cell 2004; 116: 281-297.

[10] Kos A, Olde Loohuis NF, Wieczorek ML, Glennon JC, Martens GJ, Kolk SM and Aschrafi A. A potential regulatory role for intronic microRNA-338-3p for its host gene encoding apoptosis-associated tyrosine kinase. PLoS One 2012; 7: e31022.

[11] Saba R, Goodman CD, Huzarewich RL, Robertson C and Booth SA. A miRNA signature of prion induced neurodegeneration. PLoS One 2008; 3: e3652.

[12] Huang N, Wu Z, Lin L, Zhou M, Wang L, Ma H, Xia J, Bin J, Liao Y and Liao W. MiR-338-3p inhibits epithelial-mesenchymal transition in gastric cancer cells by targeting ZEB2 and MACC1/Met/Akt signaling. Oncotarget 2015; 6: 15222-15234.

[13] Sun K, Su G, Deng H, Dong J, Lei S and Li G. Relationship between miRNA-338-3p expression and progression and prognosis of human colorectal carcinoma. Chin Med J (Engl) 2014; 127: 1884-1890.

[14] Sun J, Feng X, Gao S and Xiao Z. microRNA-338-3p functions as a tumor suppressor in human nonsmallcell lung carcinoma and targets Ras-related protein 14. Mol Med Rep 2015; 11: 1400-1406.

[15] Fu X, Tan D, Hou Z, Hu Z, Liu G, Ouyang Y and Liu F. The effect of miR-338-3p on HBx deletion-mutant (HBx-d382) mediated liver-cell proliferation through CyclinD1 regulation. PLoS One 2012; 7: e43204.

[16] Xu H, Zhao L, Fang Q, Sun J, Zhang S, Zhan C, Liu S and Zhang Y. MiR-338-3p inhibits hepatocarcinoma cells and sensitizes these cells to sorafenib by targeting hypoxia-induced factor 1alpha. PLoS One 2014; 9: e115565.

[17] Wang G, Sun Y, He Y, Ji C, Hu B and Sun Y. MicroRNA-338-3p inhibits cell proliferation in hepatocellular carcinoma by target forkhead box P4 (FOXP4). Int J Clin Exp Pathol 2015; 8: 337-344.

[18] Schepers GE, Teasdale RD and Koopman P. Twenty pairs of sox: extent, homology, and nomenclature of the mouse and human sox transcription factor gene families. Dev Cell 2002; 3: 167-170.

[19] Wegner M. From head to toes: the multiple facets of Sox proteins. Nucleic Acids Res 1999; 27: 1409-1420.

[20] Cheung M, Abu-Elmagd M, Clevers H and Scotting PJ. Roles of Sox4 in central nervous system development. Brain Res Mol Brain Res 2000; 79: 180-191.

[21] Kang M, Li Y, Liu W, Wang R, Tang A, Hao H, Liu Z and Ou H. miR-129-2 suppresses proliferation and migration of esophageal carcinoma cells through downregulation of SOX4 expression. Int J Mol Med 2013; 32: 51-58.

[22] Wang L, Li Y, Yang X, Yuan H, Li X, Qi M, Chang YW, Wang C, Fu W, Yang M, Zhang J and Han B. ERG-SOX4 interaction promotes epithelial-mesenchymal transition in prostate cancer cells. Prostate 2014; 74: 647-658.

[23] Huang HY, Cheng YY, Liao WC, Tien YW, Yang CH, Hsu SM and Huang PH. SOX4 transcriptionally regulates multiple SEMA3/plexin family members and promotes tumor growth in pancreatic cancer. PLoS One 2012; 7: e48637.

[24] Zhou Q, Wang Y, Che G, Zhu W, Chen X, Chen X and Sun Z. [Establishment and their biological characteristics of clonal cell subpopulations (NL9980 and L9981) from a human lung large cell carcinoma cell line (WCQH-9801)]. Zhongguo Fei Ai Za Zhi 2003; 6: 464-468.

[25] Li CY, Tan L, Zhang GJ, Li P, Tong C, Fan J and Zhu YS. Transcriptional regulation of urokinase receptor in high-(95D) and low-metastatic (95C) human lung cancer cells. Acta Biochim Biophys Sin (Shanghai) 2004; 36: 405-411.

[26] Liu H, Li Y, Li Y, Liu B, Wu H, Wang J, Wang Y, Wang M, Tang SC, Zhou Q and Chen J. Cloning and functional analysis of FLJ20420: a novel transcription factor for the BAG-1 promoter. PLoS One 2012; 7: e34832.

[27] Koumangoye RB, Andl T, Taubenslag KJ, Zilberman ST, Taylor CJ, Loomans HA and Andl CD. SOX4 interacts with EZH2 and HDAC3 to suppress microRNA-31 in invasive esophageal cancer cells. Mol Cancer 2015; 14: 24.

[28] Tiwari N, Tiwari VK, Waldmeier L, Balwierz PJ, Arnold P, Pachkov M, Meyer-Schaller N, Schubeler D, van Nimwegen E and Christofori G. Sox4 is a master regulator of epithelial-mesenchymal transition by controlling Ezh2 expression and epigenetic reprogramming. Cancer Cell 2013; 23: 768-783.

[29] You J, Li Y, Fang N, Liu B, Zu L, Chang R, Li X and Zhou Q. MiR-132 suppresses the migration and invasion of lung cancer cells via targeting the EMT regulator ZEB2. PLoS One 2014; 9: e91827.

[30] Liu B, Wu X, Liu B, Wang C, Liu Y, Zhou Q and Xu K. MiR-26a enhances metastasis potential of lung cancer cells via AKT pathway by targeting PTEN. Biochim Biophys Acta 2012; 1822: 1692-1704.

[31] Li P, Chen X, Su L, Li C, Zhi Q, Yu B, Sheng H, Wang J, Feng R, Cai Q, Li J, Yu Y, Yan M, Liu B and Zhu Z. Epigenetic silencing of miR-338-3p contributes to tumorigenicity in gastric cancer by targeting SSX2IP. PLoS One 2013; 8: e66782.

[32] Sun K, Deng HJ, Lei ST, Dong JQ and Li GX. miRNA-338-3p suppresses cell growth of human colorectal carcinoma by targeting smoothened. World J Gastroenterol 2013; 19: 2197-2207.

[33] Vervoort SJ, Lourenco AR, van Boxtel R and Coffer PJ. SOX4 mediates TGF-beta-induced expression of mesenchymal markers during mammary cell epithelial to mesenchymal transition. PLoS One 2013; 8: e53238.

[34] Shiota M, Itsumi M, Takeuchi A, Imada K, Yokomizo A, Kuruma H, Inokuchi J, Tatsugami K, Uchiumi T, Oda Y and Naito S. Crosstalk between EMT and castration resistance mediated by Twist1/AR signaling in prostate cancer. Endocr Relat Cancer 2015; 22: 889-900.

[35] Mitra A, Mishra L and Li S. EMT, CTCs and CSCs in tumor relapse and drug-resistance. Oncotarget 2015; 6: 10697-10711.

[36] Sakamoto S and Ichikawa T. [Mechanism of prostate cancer invasion and metastasis]. Nihon Rinsho 2014; 72: 2086-2089.

[37] Zhang J, Liang Q, Lei Y, Yao M, Li L, Gao X, Feng J, Zhang Y, Gao H, Liu DX, Lu J and Huang B. SOX4 induces epithelial-mesenchymal transition and contributes to breast cancer progression. Cancer Res 2012; 72: 4597-4608.

[38] Davis FM, Stewart TA, Thompson EW and Monteith GR. Targeting EMT in cancer: opportunities for pharmacological intervention. Trends Pharmacol Sci 2014; 35: 479-488.

[39] Kaufhold S and Bonavida B. Central role of Snail1 in the regulation of EMT and resistance in cancer: a target for therapeutic intervention. J Exp Clin Cancer Res 2014; 33: 62.

Table S1. Primers used in the paper were listed

Gene	Primer	Sequence (5'-3')
Primers for qRT-PCR		
U6	forward	CTCGCTTCGGCAGCACA
	reverse	AACGCTTCACGAATTTGCGT
MiR-338-3p	forward	GCCGATCCAGCATCAGTG
	reverse	CAGTGCAGGGTCCGAGGT
Sox4	forward	GTGAGCGAGATGATCTCGGG
	reverse	CAGGTTGGAGATGCTGGACTC
GAPDH	forward	CATCACCATCTTCCAGGAGCG
	reverse	TGACCTTGCCCACAGCCTTG
Primers for Sox4 3'UTR		
Sox4 3'UTR-wt	forward	GAGCTC CTCCGCCTTCTTTTCTAC
	reverse	CTCGAG CACGTCTTCTCATTTACACC
Sox4 3'UTR-mut	forward	TGGACGACTTTAAAAAAACAATTCAG
	reverse	CAGATTTGAGTTGCGTTTGAATC
Primers for Chip		
a (-800 bp)	forward	CCTGCCCCGCCCCAACCCT
	reverse	TGCCGTGGACTGTACCAGGTGC
b (+1 bp)	forward	GCCATGTCGTCGTCCTTCTTCAA
	reverse	TGCAAACCGGGAGCCGTG
c (+800 bp)	forward	GCCAGTCCACATTACAGAGCC
	reverse	CAGCTTGACAGCGTCACCTC